RESEARCH ARTICLE

Plasmodium falciparum-Infected Erythrocyte Knob Density Is Linked to the PfEMP1 Variant Expressed

Ramesh Subramani,[a] Katharina Quadt,[b] Anine E. Jeppesen,[a] Casper Hempel,[c] Jens Emil Vang Petersen,[a] Tue Hassenkam,[e] Lars Hviid,[a,d] Lea Barfod[a,d]

Centre for Medical Parasitology, Department of Immunology and Microbiology, Faculty of Health and Medical Sciences, University of Copenhagen, Copenhagen, Denmark[a]; Department of Infectious Diseases, University of Heidelberg, Heidelberg, Germany[b]; Department of Clinical Microbiology, Copenhagen University Hospital (Rigshospitalet), Copenhagen, Denmark[c]; Department of Infectious Diseases, Copenhagen University Hospital (Rigshospitalet), Copenhagen, Denmark[d]; Department of Chemistry, Faculty of Natural Sciences, Nano-Science Center, University of Copenhagen, Copenhagen, Denmark[e]

ABSTRACT **Members of the clonally variant *Plasmodium falciparum* erythrocyte membrane protein 1 (PfEMP1) family mediate adhesion of infected erythrocytes (IEs) to vascular receptors. PfEMP1 expression is normally confined to nanoscale knob protrusions on the IE surface membrane. To investigate the relationship between the densities of these IE surface knobs and the PfEMP1 variant expressed, we used specific antibody panning to generate three sublines of the *P. falciparum* clone IT4, which expresses the PfEMP1 variants IT4VAR04, IT4VAR32b, and IT4VAR60. The knob density in each subline was then determined by atomic force microscopy (AFM) and scanning electron microscopy (SEM) and compared to PfEMP1 and knob-associated histidine-rich protein (KAHRP) expression. Selection for uniform expression of IT4VAR04 produced little change in knob density, compared to unselected IEs. In contrast, selection for IT4VAR32b expression increased knob density approximately 3-fold, whereas IEs selected for IT4VAR60 expression were essentially knobless. When IT4VAR60$^+$ IEs were subsequently selected to express IT4VAR04 or IT4VAR32b, they again displayed low and high knob densities, respectively. All sublines expressed KAHRP regardless of the PfEMP1 expressed. Our study documents for the first time that knob density is related to the PfEMP1 variant expressed. This may reflect topological requirements to ensure optimal adhesive properties of the IEs.**

IMPORTANCE **Infections with *Plasmodium falciparum* malaria parasites are still responsible for many deaths, especially among children and pregnant women. New interventions are needed to reduce severe illness and deaths caused by this malaria parasite. Thus, a better understanding of the mechanisms behind the pathogenesis is essential. A main reason why *Plasmodium falciparum* malaria is more severe than disease caused by other malaria species is its ability to express variant antigens on the infected erythrocyte surface. These antigens are presented on membrane protrusions known as knobs. This study set out to investigate the interplay between different variant antigens on the surface of *P. falciparum*-infected erythrocytes and the density of the knobs on which the antigens are expressed. Such a direct analysis of this relationship has not been reported before but adds to the important understanding of the complexity of malaria antigen presentation.**

Received 27 August 2015 **Accepted** 28 August 2015 **Published** 6 October 2015

Citation Subramani R, Quadt K, Jeppesen AE, Hempel C, Petersen JEV, Hassenkam T, Hviid L, Barfod L. 2015. *Plasmodium falciparum*-infected erythrocyte knob density is linked to the PfEMP1 variant expressed. mBio 6(5):e01456-15. doi:10.1128/mBio.01456-15.

Editor Louis H. Miller, NIAID, NIH

Address correspondence to Lea Barfod, lea.barfod@ndm.ox.ac.uk.

Plasmodium falciparum causes the most virulent form of malaria (1). When *P. falciparum* parasites invade red blood cells, several modifications occur in the infected erythrocyte (IE), especially on its surface membrane. One important modification is the formation of nanoscale protrusions, which are known as knobs (1–5). Knobs are 50 to 120 nm in diameter and 2 to 20 nm in height (6, 7) and act as a site for anchoring *P. falciparum* erythrocyte membrane protein 1 (PfEMP1) (8). The role of PfEMP1 is to enable adhesion of IEs to various host receptors to avoid splenic clearance, and clonal antigenic variation allows IEs to evade immune recognition. IE sequestration in the brain, which has been implicated in the pathogenesis of cerebral malaria (CM), appears to involve PfEMP1 variants binding to intercellular adhesion molecule 1 (ICAM-1) and to endothelial protein C receptor (EPCR) (9–11). Similarly, placental malaria is caused by IEs expressing VAR2CSA-type PfEMP1 binding to chondroitin sulfate A (CSA) (12, 13). Rosetting is another PfEMP1-dependent IE adhesion phenotype, with IEs binding to receptors on uninfected erythrocytes. Rosetting has repeatedly been associated with severe malaria in sub-Saharan Africa (14, 15). An example of a PfEMP1 variant identified as a rosetting ligand is IT4VAR60, which is expressed by the parasite line known as FCR3S1.2/PAR$^+$ (16, 17).

Knobs contain several additional parasite-encoded proteins, such as knob-associated histidine-rich protein (KAHRP), *Plasmodium* helical interspersed subtelomeric (PHIST), PfEMP3, and mature parasite-infected erythrocyte surface antigen (MESA) (18). Unlike PfEMP1, these proteins are not exposed on the outer part of the membrane but interact with spectrin and actin in the erythrocyte cytoskeleton. KAHRP and PHIST are required for formation of knobs, but not for surface expression of PfEMP1 (19).

However, knobless IEs often display reduced rigidity and adhesiveness compared to knobby IEs (20, 21). These findings suggest that the association between PfEMP1 and knobs has important consequences for IE sequestration and that this association depends on the PfEMP1 variant expressed. However, to our knowledge, the relation between PfEMP1 variants, KAHRP expression, and knob density has not been studied in detail. Therefore, the present study was set up to do so. We used atomic force microscopy (AFM) and scanning electron microscopy (SEM) to compare knob expression in three sublines of *P. falciparum* IT4 that were selected by using variant-specific antibodies to express different PfEMP1s. The results obtained showed that knob density depends on the PfEMP1 protein expressed on the IE surface.

RESULTS

Knob density depends on the expressed PfEMP1 variant. To investigate the correlation between knob density and PfEMP1 expression, *P. falciparum* IT4 was selected by PfEMP1-specific antibodies to express three different PfEMP1 variants (IT4VAR32b, ITVAR04, and IT4VAR60). Transcription of the expected PfEMP1-encoding *var* gene was verified by quantitative reverse transcription-PCR, and expression of the corresponding PfEMP1 variant on the IE surface was documented by flow cytometry using variant-specific antibodies (Fig. 1). Antibody selection for expression of IT4VAR32b and IT4VAR04 resulted in highly dominant transcription of the expected *var* gene and exclusive IE surface expression of the corresponding PfEMP1 variant (Fig. 1a and b). Following selection for IT4VAR60$^+$ IEs, the majority of parasites transcribed *it4var60* and expressed IT4VAR60, although a minority continued to express other PfEMP1 variants (Fig. 1c). As in previous studies, we observed that erythrocytes infected by ring-stage parasites were knobless, followed by a steady increase in knob densities on the IE surface from 20 h to 35 h postinvasion (see Fig. S2 in the supplemental material), which is compatible with previously reported results (3, 6, 7). AFM analysis of the selected IEs revealed significant PfEMP1-dependent differences in IE knob density between the three sublines ($P \leq 0.001$) (Fig. 1d, e, and f). The knob density on ITVAR32b$^+$ IEs (16.4 ± 8.8 knobs/μm^2 [mean ± standard deviation]) was more than 3-fold higher ($P \leq 0.001$) than before selection (4.7 ± 1.7 knobs/μm^2) (see Fig. S1 in the supplemental material), whereas IT4VAR04$^+$ IEs had significantly fewer knobs (2.9 ± 1.6 knobs/μm^2; $P \leq 0.001$). AFM analysis of the IEs selected for expression of IT4VAR60 showed that three-quarters were knobless, while the rest were knobby with a density (3.6 ± 1.6 knobs/μm^2) that did not differ significantly from that in the unselected culture (Fig. 1f).

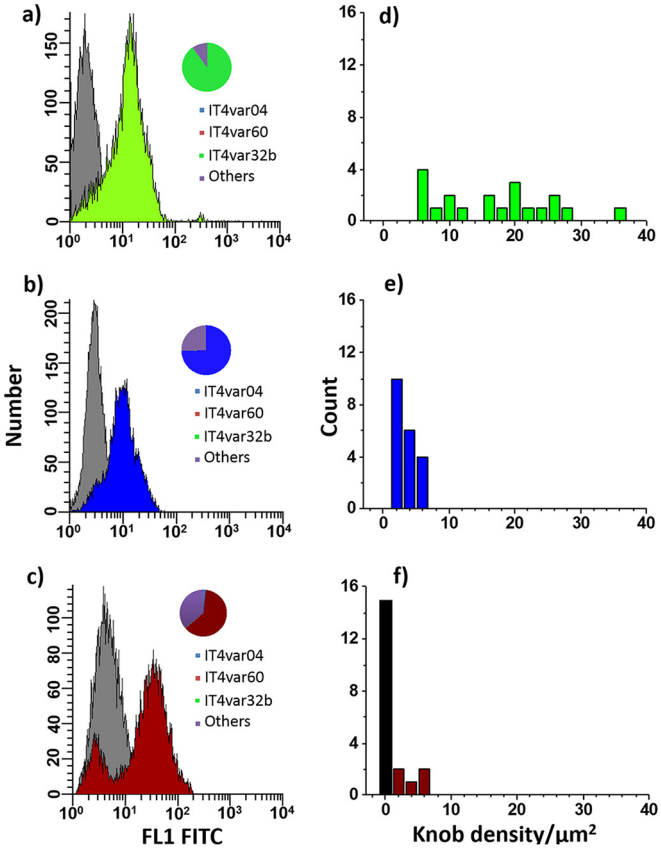

FIG 1 Expression of PfEMP1 and knobs on the surface of antibody-selected IEs. (a, b, and c) Flow cytometry histograms of antibody-selected IEs show surface reactivity with anti-IT4VAR32b (a; green), anti-IT4VAR04 (b; blue), and anti-IT4VAR60 (c; burgundy). Labeling with the negative-control antibody is shown in gray. Pie charts show the corresponding *var* gene transcription profiles. (d, e, and f) Frequency histograms showing knob densities on antibody-selected erythrocytes infected by IT4VAR32b (d), IT4VAR04 (e), and IT4VAR60 (f), measured by AFM. The black bar in panel f represents knobless IEs.

IT4VAR60$^+$ IEs are knobless. Since antibody selection of IEs for expression of IT4VAR60 did not result in uniform expression of the expected PfEMP1, we used fluorescence-activated cell sorting (FACS) to separate IT4VAR60$^+$ and IT4VAR60$^-$ IEs. The knob expression was reassessed by AFM after a few days of *in vitro* culture of the sorted IEs. Among the IEs sorted to be IT4VAR60$^+$, the large majority (85%) were knobless (Fig. 2a), while the remaining had few knobs (mean, 2.4 ± 1.0 knobs/μm^2). In marked contrast, all IEs sorted to be IT4VAR60$^-$ had knobs (Fig. 2b). Analysis of similar FACS-sorted IT4VAR60$^{+/-}$ IEs by SEM (examples are shown in Fig. 3a and b) generally confirmed the results obtained with AFM, although overall the calculated knob densities were higher (IT4VAR60$^+$, 3.4 ± 3.3 knobs/μm^2; IT4VAR60$^-$, 9.2 ± 6.3 knobs/μm^2) (Fig. 3c and d). Similar results were obtained for IT4VAR04$^+$ and IT4VAR32b$^+$ IEs (see Fig. S3 in the supplemental material). However, the numeric discrepancy between the AFM and SEM data was explained by shrinkage of leaky and osmotically fragile IEs during processing for electron microscopy (6). The estimated diameter of IEs by SEM (4.4 ± 0.4 μm) was markedly lower than the more realistic 8.0 ± 0.5 μm measured by AFM (see Fig. S4 in the supplemental material). When compensating for this shrinkage, AFM and SEM results agreed well.

The knobby phenotype reappears when knobless IT4VAR60$^+$ IEs are selected to switch PfEMP1 expression. We next investigated whether the acquisition of a knobless IE phenotype after selection for expression of IT4VAR60 was related to expression of that particular PfEMP1 variant (and therefore presumably reversible) or due to an inadvertent irreversible change (e.g., deletion of *kahrp*). The FACS-sorted IT4VAR60$^+$ culture was therefore reselected with antibodies leading to expression of either IT4VAR04 or IT4VAR32b. As before, we verified *var* gene transcription and IE surface expression profiles of the antibody-selected parasites (Fig. 4a and c). After selection for IT4VAR32b expression, a high mean knob density (24.4 ± 11.4 knobs/μm^2) was observed by

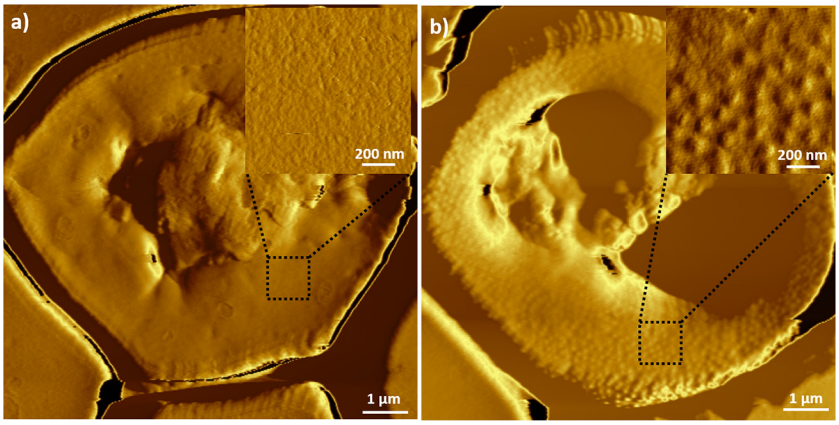

FIG 2 AFM analysis of knob expression. Representative AFM images of single IEs from IEs selected for (a) or against (b) expression of IT4VAR60 are shown. Inserts provide high-magnification details of the knobless (a) and knobby (b) surfaces. White bars indicate scales.

SEM (Fig. 4b) and resembled that of the original IT4VAR32b-selected IEs (Fig. 1d). Similarly, all IEs were knobby after selection for expression of IT4VAR04 (Fig. 4d), at a density (7.7 ± 3.7 knobs/μm^2), which was comparable to that of the original IT4VAR04-selected IEs (Fig. 1e). These results suggest that IE knob density is reversible, as shown previously (22), and depends on the PfEMP1 variant expressed on the IE surface. However, we could not exclude unintentional selection of a small subpopulation of *kahrp*-positive (and knobby) parasites from a population where most had lost this gene (which is required for knob expression) during the previous selection for expression of IT4VAR60.

The knobless phenotype of IT4VAR60$^+$ IEs is not due to loss of KAHRP expression. To assess whether the loss of knobs was associated with reduced or lost KAHRP expression, we assessed *kahrp* transcription in the parasites selected to express different PfEMP1 variants on the IE surfaces. All parasites showed comparable levels of *kahrp* transcription, regardless of PfEMP1 surface expression (Fig. 5). Furthermore, we did not observe PfEMP1-dependent differences when KAHRP expression was assessed by immunofluorescence microscopy of IEs expressing the three different PfEMP1 variants studied (Fig. 6b, f, and j). Notably, IE labeling with PfEMP1-specific antibodies resulted in a punctate surface distribution, regardless of which PfEMP1 was expressed (Fig. 6c, g, and k). Based on these data, we conclude that IE knob density depends on the PfEMP1 variant expressed on the IE surface.

DISCUSSION

Due to the importance of PfEMP1 in pathogenesis, a large number of studies have been performed on multiple aspects of PfEMP1

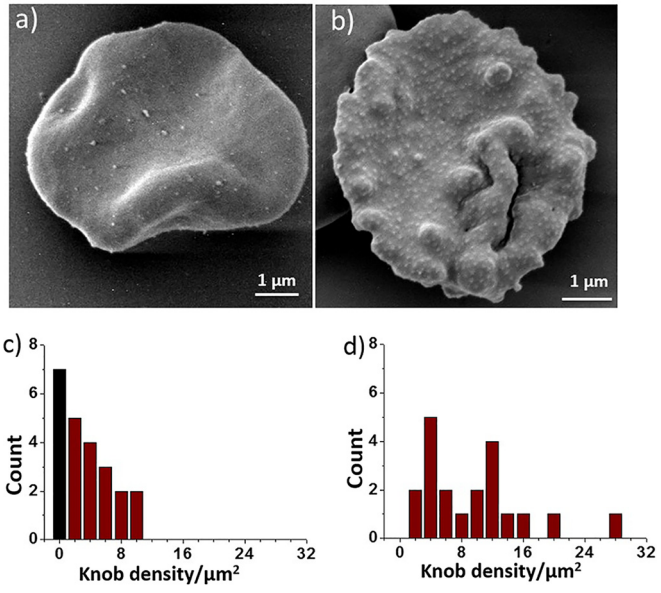

FIG 3 SEM analysis of knob expression. Representative SEM images of single IEs from populations selected for (a) or against (b) expression of IT4VAR60 are shown. Frequency histograms show knob densities on fluorescence-activated cell-sorted IT4VAR60$^-$ (c) and IT4VAR60$^+$ IEs (d). The black bar in panel c represents the result for knobless IEs.

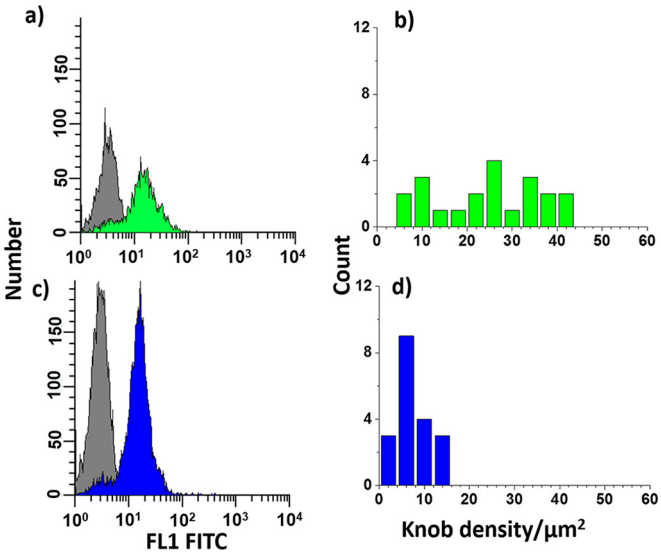

FIG 4 Expression of PfEMP1 and knobs on the IE surface following flow cytometry sorting of IEs. Flow cytometry histograms of FACS-sorted IEs show the surface reactivities with anti-IT4VAR32b (a; green) and anti-IT4VAR04 (c; blue) antibodies. Labeling with negative-control antibody is shown in gray. Frequency histograms showing knob densities on antibody-selected erythrocytes infected by IT4VAR32b (b) and IT4VAR04 (d) were measured by AFM.

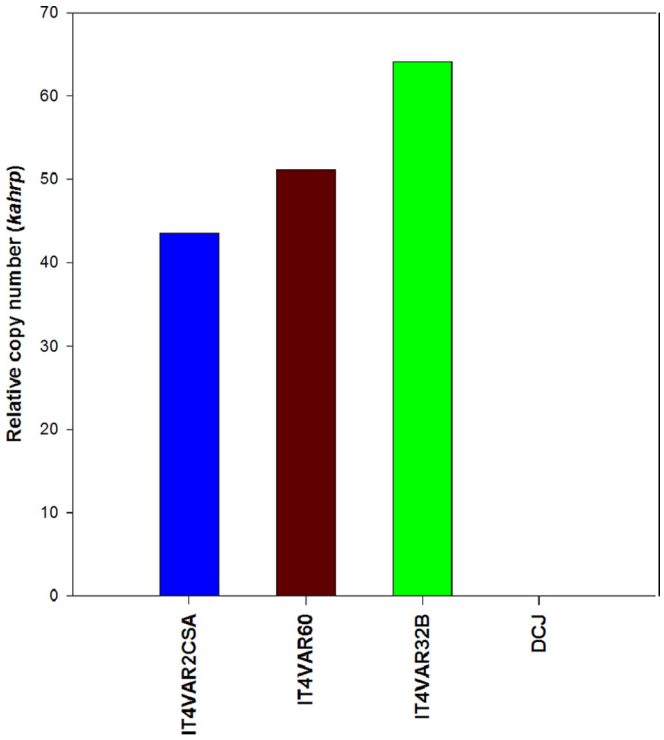

FIG 5 KAHRP transcription in antibody-selected parasites. The bar chart shows *kahrp* gene copy numbers, relative to that for the seryl-tRNA-synthetase housekeeping gene, in differently selected parasite lines. DCJ is a negative-control parasite line that has a deletion in the *kahrp* gene.

and the *var* genes that encode them (23, 24). Studies on the density of knobs on the *P. falciparum* IE surface from both *ex vivo* field isolates and *in vitro* laboratory *P. falciparum* cultures have also been done (7). However, no studies have addressed whether knob densities might depend on the specific PfEMP1 expressed. While IE knobs are seen in several *Plasmodium* species other than *P. falciparum*, including *P. malariae*, *P. brasilianum* (25), *P. fragile* (26), and *P. coatneyi* (4), PfEMP1-type IE surface proteins have only been described in *P. falciparum* and its close relative, *P. reichenowi* (27). Thus, knobs and PfEMP1 expression might be evolutionarily unrelated phenotypes, as is the ability to sequester in the host microvasculature, since other *Plasmodium* species, like *P. vivax*, *P. berghei*, and *P. chabaudi*, do sequester without having either knobs or PfEMP1-like proteins. Those *Plasmodium* species sequester using other families of variant surface antigens (28–30).

With respect to *P. falciparum*, we have shown here that knob densities appear linked to the PfEMP1 variant expressed on the knobs. This could reflect variant-specific requirements for presentation and organization of PfEMP1 on the IE surface to ensure optimal host receptor affinity. Thus, some IEs have a reduced adhesion capacity in the absence of knobs (20, 31), whereas the presence or absence of knobs does not seem to affect others, such as IT4VAR60$^+$ IEs, which form rosettes even though they do not have knobs (17). This could reflect dissimilarities in availability of the human host receptors and the force of the blood flow in the different organs in which adhesion occurs. Both IT4VAR04 and IT4VAR60 bind to receptors (CSA and uninfected erythrocytes, respectively) that are very abundant, and the speed of blood flow in the placenta is very slow. Adhesion to low-frequency receptors, on the other hand, in organs with high-speed blood flow may necessitate better presentation of parasite antigens, thus requiring a higher frequency of knobs.

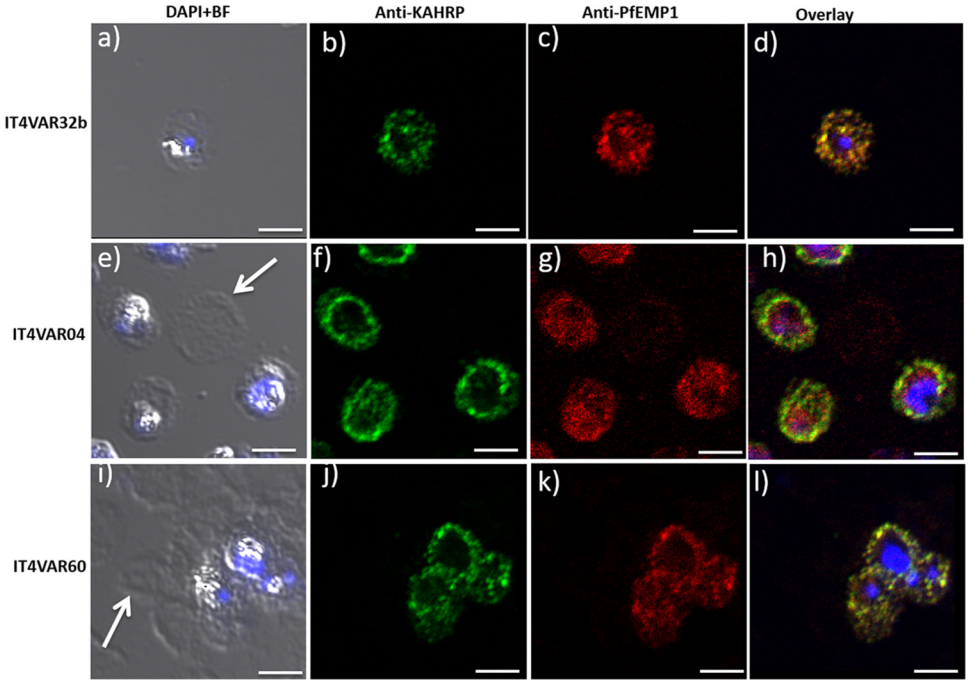

FIG 6 KAHRP and PFEMP1 protein expression on IEs. Confocal immunofluorescence microscopy images of erythrocytes infected by IT4VAR32b (a to d), IT4VAR04 (e to h), or IT4VAR60 (i to l), stained with DAPI (a, e, and i), anti-KAHRP (b, f, and j), or anti-PfEMP1 (c, g, and k) and overlays (d, h, and l). White arrows (e and i) mark uninfected erythrocytes. Scale bars, 5 μm.

The distribution of PfEMP1 molecules on the IE surface is not dependent on knobs, since the PfEMP1 molecules remain organized in clusters whether knobs are present or not (31). This most likely reflects the interaction of the intracellular part of PfEMP1 to the actin skeleton and PHIST (32, 33), and our observations of punctate PfEMP1 fluorescence in both knobby and knobless IEs are in agreement with this idea.

Parasites with a deletion or rearrangement of the *kahrp* gene do not have knobs (20, 34). However, as our knobless IT4VAR60$^+$ IEs did express KAHRP, other factors clearly impact the phenotype. As an example, PHIST proteins can bind to the cytoplasmic tail (exon 2) of PfEMP1 proteins (32). Exon 2 is highly conserved, although polymorphisms do exist, and small differences in the *exon2* sequence could potentially influence the capacity to bind PHIST and thereby impact the formation of knobs. The PfEMP1 variants we studied here represent three different exon 2 types, namely, A1, B, and E (35), but whether there is a systematic difference in knob density between the different ATS types will require further investigation. In general, better knowledge of the interaction, transportation, and regulation of these proteins involved in pathogenesis of malaria is still needed. This information will aid in the development of protective vaccines or other interventions against severe *P. falciparum* malaria.

MATERIALS AND METHODS

Antisera and monoclonal antibodies. The full-length recombinant IT4VAR60 protein used for immunization was produced in *Baculovirus*-infected insect cells, essentially as described elsewhere (36, 37). The anti-IT4VAR60 antisera were raised in rabbits as described by Stevenson et al. (38). The human monoclonal IgG antibodies AB01 (specific for IT4VAR32b) and PAM1.4 (specific for several VAR2CSA-type PfEMP1 variants, including IT4VAR04) were generated essentially as described previously (39). The KAHRP antibody (40) was a kind gift from Diane Taylor, University of Hawaii.

Malaria parasite culture, *in vitro* selection, and flow cytometry analysis of PfEMP1 surface expression. We used the long-term *in vitro*-cultured *P. falciparum* line FCR3/IT4 (41), grown in O Rh$^+$ erythrocytes without human serum (42). The initial selection of the *P. falciparum* IT4 IEs to display specific PfEMP1 proteins on the surface consisted of three rounds of panning of the IEs with rabbit antisera against full-length IT4VAR60 (43) or with human monoclonal antibodies specific for IT4VAR04 (39) or IT4VAR32b bound to protein A-coupled Dynabeads (Invitrogen), essentially as described previously (44). The phenotypes were maintained by subsequent regular selection in the same way. Antibody reactivity with IE surface antigens was assessed by flow cytometry, essentially as described previously (45). In brief, IEs were enriched for those infected by hemozoin-containing mature parasites by exposure to a strong magnetic field, using CS columns on a VarioMACS instrument (Miltenyi Biotec, Lund, Sweden) and labeled with ethidium bromide and monoclonal antibody or antiserum, followed by appropriate fluorescein isothiocyanate (FITC)-conjugated secondary antibodies. Fluorescence list-mode data were collected on an FC500 flow cytometer (Beckman Coulter), and IE surface labeling was quantified by using the WinList software (Verity Software House, Topsham, ME, USA). The selection steps are summarized in Fig. S5 in the supplemental material.

Sorting of IEs by flow cytometry. We used fluorescence-activated cell sorting (FACSAria or FACSJazz; BD Biosciences) to separate IT4VAR60-positive and -negative IEs in the antibody-panned cultures (see Fig. S5 in the supplemental material). Late-stage-infected IEs were enriched as described above and labeled with IT4VAR60 antisera, followed by appropriate FITC-conjugated secondary antibodies. Gates for the negative and positive populations were set based on the negative-control samples (labeled with secondary antibody only), with a gap to ensure no overlap between the two sorted populations.

Analysis of knob densities via AFM. Knob densities on IEs were measured by AFM essentially as described by Quadt et al. (7). AFM images were captured either with an MFP-3D microscope (Asylum Research, Santa Barbara, CA, USA) or a Multimode8 AFM (Bruker Nano Inc., Santa Barbara, CA, USA). We used copper grids to locate the IEs via an integrated optical microscope. Images were captured in air under ambient conditions with tapping mode and using a silicon microcantilever (OMCL-AC160TS-W2; Olympus) with a spring constant of 42 N/m and a resonant frequency of ~300 kHz. The images were 512 by 512 pixels and captured at scan speeds of 0.5 to 2.0 Hz, depending on the scan size (0.25 to 15 μm). Scan speeds were optimized individually to minimize noise and integral and proportional gains.

Analysis of knob densities via SEM. SEM was used on late-stage IEs obtained as described above. The IEs were initially fixed in glutaraldehyde (2% in phosphate-buffered saline [PBS]; 30 min, room temperature) and washed in PBS. The IEs were then transferred to pretreated poly-L-lysine-coated coverslips, washed in PBS, and dehydrated by using a standard ethanol protocol (21). Finally, the IEs were subjected to critical point drying (CPD030; Bal-Tech, Balzers, Liechtenstein), coated with gold in a sputter coater, and viewed in a Philips XL30 FEG scanning electron microscope at 2 kV (Core Facility for Integrated Microscopy [CFIM], Faculty of Health Sciences, University of Copenhagen, Copenhagen, Denmark).

Detection of KAHRP by confocal microscopy. For immunofluorescence assays, magnetically activated cell sorter (MACS)-purified late-stage IEs were surface labeled with PfEMP1-specific antibodies as described by Bengtsson et al. (46). Next, 10-μl aliquots of IEs were transferred to poly-L-lysine-coated coverslips and fixed with paraformaldehyde (4% in PBS; 20 min) and then rinsed twice with PBS. The samples were treated with 0.5% Triton X-100 for 5 min and blocked with 10% bovine serum albumin (1 h, 4°C). Thereafter, KAHRP antibody labeling was performed (46) using Alexa 564-conjugated anti-mouse IgG (Invitrogen, Life Technologies) and gold antifade reagent with 4′,6-diamidino-2-phenylindole (DAPI; Invitrogen, Life Technologies). IEs were examined with a Nikon Eclipse TE 2000-E microscope with a 60× oil immersion objective lens. Laser intensity and gain settings were adjusted manually and kept the same for all IEs, to enable direct comparisons. Captured images were processed using the EZ-C1 viewer software (Nikon, Birkerød, Denmark). Final image sizes were 25 μm by 25 μm.

RNA transcription analysis. Analysis of *var* gene transcription by quantitative real-time PCR was done using cDNA generated from ring-stage parasite RNA and *P. falciparum kahrp* and *var* gene-specific primers as described in detail elsewhere (47, 48). The primers used, modified to increase specificity to the target genes, were as follows: *it4var19* forward, GGGAGCTCAGAAAGTGGTAA; *it4var19* reverse, TGTTCGTCG TCATCTTCAAC; *it4var32a* forward, GTACTGGTGGTGTTGCAAAT; *it4var32a* reverse, TCCTCGTCCTCTTCCTTTAC; *it4var32b* forward, CC AGGCAAAACTAGTGACAG; *it4var32b* reverse, CTGGTTTACAACCG TCTTTG. The amplification efficiencies of the modified primers on 10-fold dilutions of genomic DNA were comparable to those of the reference seryl-tRNA-synthetase primers. Melting curves for the primers and transcripts each had a single defined peak. Transcription levels relative to the housekeeping gene for seryl-tRNA synthetase were calculated using the $2^{-\Delta CT}$ method. The *P. falciparum* parasite DC-J (49), which has a deletion of the *karhp* gene (50), was used as a negative control for *karhp* transcription.

Statistics. All statistical analyses were performed using SigmaPlot 12.5. Related and unrelated data sets passing an initial Shapiro-Wilk normality test were compared by one-way analysis of variance tests and *t* tests, respectively. Otherwise, Kruskal-Wallis tests or Mann-Whitney U tests were used.

SUPPLEMENTAL MATERIAL

Supplemental material for this article may be found at http://mbio.asm.org/lookup/suppl/doi:10.1128/mBio.01456-15/-/DCSupplemental.

Figure S1, TIF file, 0.6 MB.
Figure S2, TIF file, 0.6 MB.
Figure S3, PNG file, 0.02 MB.
Figure S4, TIF file, 2 MB.
Figure S5, TIF file, 0.1 MB.

ACKNOWLEDGMENTS

Kirsten Pihl Zimling, Maiken Visti, and Michele P. Kreutzer are thanked for excellent technical assistance.

This work was supported by grants from the Danish Medical Research Council (DFF-FSS, grants 11-120879 and 11-115707), the Lundbeck Foundation (grants R9-A840, R48-A4847, and R83-A7627), the Novo Nordisk Foundation ("Immune evasion of malaria parasites: binding of non-immune IgM to infected erythrocytes"), and the University of Copenhagen (Programme of Excellence in Membrane Topology and Quaternary Structure of Key Membrane Proteins Involved in Plasmodium falciparum Malaria Pathogenesis and Immunity and "CoNeXT—Fertilizing the ground and harvesting the full potential of the new neutron and X-ray research infrastructures close to Copenhagen University").

We have no conflicting financial interests.

REFERENCES

1. **Li A, Mansoor AH, Tan KS, Lim CT**. 2006. Observations on the internal and surface morphology of malaria infected blood cells using optical and atomic force microscopy. J Microbiol Methods **66:**434–439. http://dx.doi.org/10.1016/j.mimet.2006.01.009.
2. **Shi H, Liu Z, Li A, Yin J, Chong AG, Tan KS, Zhang Y, Lim CT**. 2013. Life cycle-dependent cytoskeletal modifications in *Plasmodium falciparum* infected erythrocytes. PLoS One **8:**e61170. http://dx.doi.org/10.1371/journal.pone.0061170.
3. **Nagao E, Kaneko O, Dvorak JA**. 2000. *Plasmodium falciparum*-infected erythrocytes: qualitative and quantitative analyses of parasite-induced knobs by atomic force microscopy. J Struct Biol **130:**34–44. http://dx.doi.org/10.1006/jsbi.2000.4236.
4. **Luse SA, Miller LH**. 1971. *Plasmodium falciparum* malaria. Ultrastructure of parasitized erythrocytes in cardiac vessels. Am J Trop Med Hyg **20:**655–660.
5. **Miller LH**. 1972. The ultrastructure of red cells infected by *Plasmodium falciparum* in man. Trans R Soc Trop Med Hyg **66:**459–462. http://dx.doi.org/10.1016/0035-9203(72)90277-5.
6. **Gruenberg J, Allred DR, Sherman IW**. 1983. Scanning electron microscope-analysis of the protrusions (knobs) present on the surface of *Plasmodium falciparum*-infected erythrocytes. J Cell Biol **97:**795–802. http://dx.doi.org/10.1083/jcb.97.3.795.
7. **Quadt KA, Barfod L, Andersen D, Bruun J, Gyan B, Hassenkam T, Ofori MF, Hviid L**. 2012. The density of knobs on *Plasmodium falciparum*-infected erythrocytes depends on developmental age and varies among isolates. PLoS One **7:**e45658. http://dx.doi.org/10.1371/journal.pone.0045658.
8. **Smith JD, Rowe JA, Higgins MK, Lavstsen T**. 2013. Malaria's deadly grip: cytoadhesion of *Plasmodium falciparum*-infected erythrocytes. Cell Microbiol **15:**1976–1983. http://dx.doi.org/10.1111/cmi.12183.
9. **Turner L, Lavstsen T, Berger SS, Wang CW, Petersen JE, Avril M, Brazier AJ, Freeth J, Jespersen JS, Nielsen MA, Magistrado P, Lusingu J, Smith JD, Higgins MK, Theander TG**. 2013. Severe malaria is associated with parasite binding to endothelial protein C receptor. Nature **498:**502–505. http://dx.doi.org/10.1038/nature12216.
10. **Turner GD, Morrison H, Jones M, Davis TM, Looareesuwan S, Buley ID, Gatter KC, Newbold CI, Pukritayakamee S, Nagachinta B, White NJ, Berendt AR**. 1994. An immunohistochemical study of the pathology of fatal malaria: evidence for widespread endothelial activation and a potential role for intercellular adhesion molecule-1 in cerebral sequestration. Am J Pathol **145:**1057–1069.
11. **Newbold C, Warn P, Black G, Berendt A, Craig A, Snow B, Msobo M, Peshu N, Marsh K**. 1997. Receptor-specific adhesion and clinical disease in *Plasmodium falciparum*. Am J Trop Med Hyg **57:**389–398.
12. **Salanti A, Staalsoe T, Lavstsen T, Jensen AT, Sowa MP, Arnot DE, Hviid L, Theander TG**. 2003. Selective upregulation of a single distinctly structured *var* gene in chondroitin sulphate-adhering *Plasmodium falciparum* involved in pregnancy-associated malaria. Mol Microbiol **49:**179–191. http://dx.doi.org/10.1046/j.1365-2958.2003.03570.x.
13. **Salanti A, Dahlbäck M, Turner L, Nielsen MA, Barfod L, Magistrado P, Jensen AT, Lavstsen T, Ofori MF, Marsh K, Hviid L, Theander TG**. 2004. Evidence for the involvement of VAR2CSA in pregnancy-associated malaria. J Exp Med **200:**1197–1203. http://dx.doi.org/10.1084/jem.20041579.
14. **Rowe A, Obeiro J, Newbold CI, Marsh K**. 1995. *Plasmodium falciparum* rosetting is associated with malaria severity in Kenya. Infect Immun **63:**2323–2326.
15. **Doumbo OK, Thera MA, Koné AK, Raza A, Tempest LJ, Lyke KE, Plowe CV, Rowe JA**. 2009. High levels of *Plasmodium falciparum* rosetting in all clinical forms of severe malaria in African children. Am J Trop Med Hyg **81:**987–993. doihttp://dx.doi.org/10.4269/ajtmh.2009.09-0406.
16. **Albrecht L, Moll K, Blomqvist K, Normark J, Chen Q, Wahlgren M**. 2011. *var* gene transcription and PfEMP1 expression in the rosetting and cytoadhesive *Plasmodium falciparum* clone FCR3S1.2. Malar J **10:**17. http://dx.doi.org/10.1186/1475-2875-10-17.
17. **Udomsangpetch R, Aikawa M, Berzins K, Wahlgren M, Perlmann P**. 1989. Cytoadherence of knobless *Plasmodium falciparum*-infected erythrocytes and its inhibition by a human monoclonal antibody. Nature **338:**763–765. http://dx.doi.org/10.1038/338763a0.
18. **Cooke BM, Glenister FK, Mohandas N, Coppel RL**. 2002. Assignment of functional roles to parasite proteins in malaria-infected red blood cells by competitive flow-based adhesion assay. Br J Haematol **117:**203–211. http://dx.doi.org/10.1046/j.1365-2141.2002.03404.x.
19. **Maier AG, Rug M, O'Neill MT, Brown M, Chakravorty S, Szestak T, Chesson J, Wu Y, Hughes K, Coppel RL, Newbold C, Beeson JG, Craig A, Crabb BS, Cowman AF**. 2008. Exported proteins required for virulence and rigidity of *Plasmodium falciparum*-infected human erythrocytes. Cell **134:**48–61. http://dx.doi.org/10.1016/j.cell.2008.04.051.
20. **Crabb BS, Cooke BM, Reeder JC, Waller RF, Caruana SR, Davern KM, Wickham ME, Brown GV, Coppel RL, Cowman AF**. 1997. Targeted gene disruption shows that knobs enable malaria-infected red cells to cytoadhere under physiological shear stress. Cell **89:**287–296. http://dx.doi.org/10.1016/S0092-8674(00)80207-X.
21. **Rug M, Prescott SW, Fernandez KM, Cooke BM, Cowman AF**. 2006. The role of KAHRP domains in knob formation and cytoadherence of *P. falciparum*-infected human erythrocytes. Blood **108:**370–378. http://dx.doi.org/10.1182/blood-2005-11-4624.
22. **Gritzmacher CA, Reese RT**. 1984. Reversal of knob formation on *Plasmodium falciparum*-infected erythrocytes. Science **226:**65–67. http://dx.doi.org/10.1126/science.6382613.
23. **Hviid L, Jensen AT**. 2015. PfEMP1—a parasite protein family of key importance in *Plasmodium falciparum* malaria immunity and pathogenesis. Adv Parasitol **88:**51–84. http://dx.doi.org/10.1016/bs.apar.2015.02.004.
24. **Kraemer SM, Smith JD**. 2006. A family affair: *var* genes, PfEMP1 binding, and malaria disease. Curr Opin Microbiol **9:**374–380. http://dx.doi.org/10.1016/j.mib.2006.06.006.
25. **Aikawa M**. 1988. Morphological changes in erythrocytes induced by malarial parasites. Biol Cell **64:**173–181. http://dx.doi.org/10.1016/0248-4900(88)90077-9.
26. **Fujioka H, Millet P, Maeno Y, Nakazawa S, Ito Y, Howard RJ, Collins WE, Aikawa M**. 1994. A nonhuman primate model for human cerebral malaria: rhesus monkeys experimentally infected with *Plasmodium fragile*. Exp Parasitol **78:**371–376. http://dx.doi.org/10.1006/expr.1994.1040.
27. **Zilversmit MM, Chase EK, Chen DS, Awadalla P, Day KP, McVean G**. 2013. Hypervariable antigen genes in malaria have ancient roots. BMC Evol Biol **13:**110. http://dx.doi.org/10.1186/1471-2148-13-110.
28. **Franke-Fayard B, Fonager J, Braks A, Khan SM, Janse CJ**. 2010. Sequestration and tissue accumulation of human malaria parasites: can we learn anything from rodent models of malaria? PLoS Pathog **6:**e1001032. http://dx.doi.org/10.1371/journal.ppat.1001032.
29. **Lopes SC, Albrecht L, Carvalho BO, Siqueira AM, Thomson-Luque R, Nogueira PA, Fernandez-Becerra C, Del Portillo HA, Russell BM, Rénia L, Lacerda MV, Costa FT**. 2014. Paucity of *Plasmodium vivax* mature schizonts in peripheral blood is associated with their increased cytoadhesive potential. J Infect Dis **209:**1403–1407. http://dx.doi.org/10.1093/infdis/jiu018.
30. **Gilks CF, Walliker D, Newbold CI**. 1990. Relationships between seques-

tration, antigenic variation and chronic parasitism in *Plasmodium chabaudi chabaudi*—a rodent malaria model. Parasite Immunol **12:**45–64. http://dx.doi.org/10.1111/j.1365-3024.1990.tb00935.x.

31. **Horrocks P, Pinches RA, Chakravorty SJ, Papakrivos J, Christodoulou Z, Kyes SA, Urban BC, Ferguson DJ, Newbold CI.** 2005. PfEMP1 expression is reduced on the surface of knobless *Plasmodium falciparum* infected erythrocytes. J Cell Sci **118:**2507–2518. http://dx.doi.org/10.1242/jcs.02381.
32. **Mayer C, Slater L, Erat MC, Konrat R, Vakonakis I.** 2012. Structural analysis of the *Plasmodium falciparum* erythrocyte membrane protein 1 (PfEMP1) intracellular domain reveals a conserved interaction epitope. J Biol Chem **287:**7182–7189. http://dx.doi.org/10.1074/jbc.M111.330779.
33. **Oberli A, Slater LM, Cutts E, Brand F, Mundwiler-Pachlatko E, Rusch S, Masik MF, Erat MC, Beck HP, Vakonakis I.** 2014. A *Plasmodium falciparum* PHIST protein binds the virulence factor PfEMP1 and comigrates to knobs on the host cell surface. FASEB J **28:**4420–4433. http://dx.doi.org/10.1096/fj.14-256057.
34. **Pologe LG, Ravetch JV.** 1986. A chromosomal rearrangement in a *P. falciparum* histidine-rich protein gene is associated with the knobless phenotype. Nature **322:**474–477. http://dx.doi.org/10.1038/322474a0.
35. **Kraemer SM, Kyes SA, Aggarwal G, Springer AL, Nelson SO, Christodoulou Z, Smith LM, Wang W, Levin E, Newbold CI, Myler PJ, Smith JD.** 2007. Patterns of gene recombination shape *var* gene repertoires in *Plasmodium falciparum*: comparisons of geographically diverse isolates. BMC Genomics **8:**45. http://dx.doi.org/10.1186/1471-2164-8-45.
36. **Barfod L, Nielsen MA, Turner L, Dahlbäck M, Jensen AT, Hviid L, Theander TG, Salanti A.** 2006. *Baculovirus*-expressed constructs induce immunoglobulin G that recognizes VAR2CSA on *Plasmodium falciparum*-infected erythrocytes. Infect Immun **74:**4357–4360. http://dx.doi.org/10.1128/IAI.01617-05.
37. **Ampomah P, Stevenson L, Ofori MF, Barfod L, Hviid L.** 2014. B-cell responses to pregnancy-restricted and -unrestricted *Plasmodium falciparum* erythrocyte membrane protein 1 (PfEMP1) antigens in Ghanaian women naturally exposed to malaria parasites. Infect Immun **82:**1860–1871. http://dx.doi.org/10.1128/IAI.01514-13.
38. **Stevenson L, Huda P, Jeppesen A, Laursen E, Rowe JA, Craig A, Streicher W, Barfod L, Hviid L.** 2015. Investigating the function of F_c-specific binding of IgM to *Plasmodium falciparum* erythrocyte membrane protein 1 mediating erythrocyte rosetting. Cell Microbiol **17:**819–831. http://dx.doi.org/10.1111/cmi.12403.
39. **Barfod L, Bernasconi NL, Dahlbäck M, Jarrossay D, Andersen PH, Salanti A, Ofori MF, Turner L, Resende M, Nielsen MA, Theander TG, Sallusto F, Lanzavecchia A, Hviid L.** 2007. Human pregnancy-associated malaria-specific B cells target polymorphic, conformational epitopes in VAR2CSA. Mol Microbiol **63:**335–347. http://dx.doi.org/10.1111/j.1365-2958.2006.05503.x.
40. **Acharya P, Chaubey S, Grover M, Tatu U.** 2012. An exported heat shock protein 40 associates with pathogenesis-related knobs in *Plasmodium falciparum* infected erythrocytes. PLoS One **7:**e44605. http://dx.doi.org/10.1371/journal.pone.0044605.
41. **Roberts DJ, Craig AG, Berendt AR, Pinches R, Nash G, Marsh K, Newbold CI.** 1992. Rapid switching to multiple antigenic and adhesive phenotypes in malaria. Nature **357:**689–692. http://dx.doi.org/10.1038/357689a0.
42. **Cranmer SL, Magowan C, Liang J, Coppel RL, Cooke BM.** 1997. An alternative to serum for cultivation of *Plasmodium falciparum in vitro*. Trans R Soc Trop Med Hyg **91:**363–365. http://dx.doi.org/10.1016/S0035-9203(97)90110-3.
43. **Stevenson L, Laursen E, Cowan GJ, Bandoh B, Barfod L, Cavanagh DR, Andersen GR, Hviid L.** 2015. α_2-Macroglobulin can crosslink multiple *Plasmodium falciparum* erythrocyte membrane protein 1 (PfEMP1) molecules and may facilitate adhesion of parasitized erythrocytes. PLoS Pathog **11:**e1005022. http://dx.doi.org/10.1371/journal.ppat.1005022.
44. **Soerli J, Barfod L, Lavstsen T, Bernasconi NL, Lanzavecchia A, Hviid L.** 2009. Human monoclonal IgG selection of *Plasmodium falciparum* for the expression of placental malaria-specific variant surface antigens. Parasite Immunol **31:**341–346. http://dx.doi.org/10.1111/j.1365-3024.2009.01097.x.
45. **Staalsø T, Khalil EA, Elhassan IM, Zijlstra EE, Elhassan AM, Giha HA, Theander TG, Jakobsen PH.** 1998. Antibody reactivity to conserved linear epitopes of *Plasmodium falciparum* erythrocyte membrane protein 1 (PfEMP1). Immunol Lett **60:**121–126. http://dx.doi.org/10.1016/S0165-2478(97)00143-0.
46. **Bengtsson D, Sowa KM, Salanti A, Jensen AT, Joergensen L, Turner L, Theander TG, Arnot DE.** 2008. A method for visualizing surface-exposed and internal PfEMP1 adhesion antigens in *Plasmodium falciparum* infected erythrocytes. Malar J **7:**101. http://dx.doi.org/10.1186/1475-2875-7-101.
47. **Wang CW, Lavstsen T, Bengtsson DC, Magistrado PA, Berger SS, Marquard AM, Alifrangis M, Lusingu JP, Theander TG, Turner L.** 2012. Evidence for *in vitro* and *in vivo* expression of the conserved VAR3 (type 3) *Plasmodium falciparum* erythrocyte membrane protein 1. Malar J **11:**129. http://dx.doi.org/10.1186/1475-2875-11-129.
48. **Amulic B, Salanti A, Lavstsen T, Nielsen MA, Deitsch KW.** 2009. An upstream open reading frame controls translation of *var2csa*, a gene implicated in placental malaria. PLoS Pathog **5:**e1000256. http://dx.doi.org/10.1371/journal.ppat.1000256.
49. **Dzikowski R, Frank M, Deitsch K.** 2006. Mutually exclusive expression of virulence genes by malaria parasites is regulated independently of antigen production. PLoS Pathog **2:**e22. http://dx.doi.org/10.1371/journal.ppat.0020022.
50. **Baratin M, Roetynck S, Pouvelle B, Lemmers C, Viebig NK, Johansson S, Bierling P, Scherf A, Gysin J, Vivier E, Ugolini S.** 2007. Dissection of the role of PfEMP1 and ICAM-1 in the sensing of *Plasmodium falciparum*-infected erythrocytes by natural killer cells. PLoS One **2:**e228. http://dx.doi.org/10.1371/journal.pone.0000228.